

Nonet Classification of Scalar/Isoscalar Resonances below 1900 MeV: the Existence of an Extra Scalar State in the Region 1200-1600 MeV

V.V. Anisovich^{a1}, Yu.D. Prokoshkin^{b2}, and A.V. Sarantsev^{a3}

Abstract

A classification of the $IJ^{PC} = 00^{++}$ mesons is performed on the basis of the K-matrix analysis of meson spectra in the reactions: (i) GAMS data on $\pi p \rightarrow \pi^0 \pi^0 n$, $\eta \eta n$, $\eta \eta' n$ [1, 2, 3]; (ii) Crystal Barrel data on $p\bar{p}$ (*at rest*) $\rightarrow \pi^0 \pi^0 \pi^0$, $\pi^0 \pi^0 \eta$, $\pi^0 \eta \eta$ [4, 5]; (iii) CERN-Münich data on $\pi p \rightarrow \pi^+ \pi^- n$ [6]; (iiii) BNL data on $\pi N \rightarrow K \bar{K} N$ [7]. The analysis points to the existence of four comparatively narrow scalar resonances which correspond to the following poles of the scattering amplitude (in MeV): $(1015 \pm 15) - i(43 \pm 8)$, $(1300 \pm 20) - i(120 \pm 20)$, $(1499 \pm 8) - i(65 \pm 10)$ and $(1780 \pm 30) - i(125 \pm 70)$. The scattering amplitude also has a fifth pole $f_0(1530^{+90}_{-250})$ at the complex mass $(1530^{+90}_{-250}) - i(560 \pm 140)$. The masses of the K-matrix poles (bare states) are at 720 ± 100 MeV, 1230 ± 50 MeV, 1260 ± 30 MeV, 1600 ± 50 MeV and 1810 ± 30 MeV. The quark content of the bare states is analyzed using the values of their couplings to the $\pi\pi$, $K\bar{K}$, $\eta\eta$ and $\eta\eta'$. It is shown that one of the bare states in the mass region 1200-1600 MeV is superfluous for the $q\bar{q}$ classification and should be considered as the lightest glueball.

a) *St.Petersburg Nuclear Physics Institute, Gatchina, 188350 Russia*

b) *Institute for High Energy Physics, Protvino, 142284 Russia*

1) anisovic@lnpi.spb.su, anisovic@thd.pnpi.spb.ru

2) prokoshkin@mx.ihep.su, Yuri.Prokoshkin@cern.ch

4) vsv@hep486.pnpi.spb.ru, andsar@v2.rl.ac.uk

The search for and classification of scalar/isoscalar $IJ^{PC} = 00^{++}$ states is the direct and possibly the only way for identification of the lightest scalar glueball. In refs. [8, 9] the K-matrix analysis of the 00^{++} -wave was performed in the mass region up to 1550 MeV, where four scalar resonances (the T-matrix poles at the complex masses: $(1008 \pm 10) - i(43 \pm 5)$, $(1290 \pm 25) - i(120 \pm 15)$, $(1497 \pm 6) - i(61 \pm 5)$, $(1430 \pm 150) - i(600 \pm 100)$, in MeV) were found. Correspondingly, four bare states were determined: the lightest bare state with mass 750 ± 100 MeV is dominantly $s\bar{s}$, while three other states, with masses 1240 ± 30 MeV, 1280 ± 30 MeV and 1615 ± 50 MeV, do not contain a large $s\bar{s}$ component. One of these states, either the state with mass 1240 MeV or the state with mass 1280 MeV, is a natural $q\bar{q}$ -partner of the lightest bare state. For the other two states two scenarios arose in ref. [9]:

- (a) both these states are $q\bar{q}$ mesons; then, in the region 1550-1900 MeV, two $s\bar{s}$ -rich states exist as the nonet partners of the low-lying 00^{++} -mesons;
- (b) in the region 1550-1900 MeV there is only one $s\bar{s}$ -rich 00^{++} state; then one of the low-lying states is exotic, probably the lightest glueball.

To resolve these alternatives, the spectra in $K\bar{K}$, $\eta\eta$ and $\eta\eta'$ channels need to be investigated in the region 1550-1900 MeV: the existence of a strange component in these mesons favours a search for the $s\bar{s}$ -rich states. The $\eta\eta$ and $\eta\eta'$ spectra obtained by the GAMS collaboration [2, 3] give a good opportunity for this study. The aim here is to extend the analysis of the 00^{++} -wave to a mass of 1900 MeV, including the $\eta\eta$ and $\eta\eta'$ GAMS spectra into the simultaneous fitting procedure. The main purpose is to identify the $s\bar{s}$ -rich states: the analysis of the $\pi^0\pi^0$ and $\pi^+\pi^-$ spectra from refs. [9, 10] definitely indicates that in the region 1550-1900 MeV there are no 00^{++} resonances with a significant $\pi\pi$ branching ratio: so, the presence of $n\bar{n}$ -dominant states is unlikely here. As to $s\bar{s}$ -rich states, the radiative J/ψ decays hint at the possible existence of a scalar resonance near 1750 MeV [11].

Lattice QCD calculations predict the mass of the purely gluonic 0^{++} state (glueball) in the region 1500-1750 MeV: 1550 ± 50 MeV [12] and 1707 ± 64 MeV [13]. However, if the glueball is near 1500 MeV, it must definitely include quark degrees of freedom, mainly the $q\bar{q}$ -component. Quark-antiquark loop diagrams (Fig. 1a) will reduce the mass of a pure glueball: the mass shift is of the order of 100-300 MeV [14]. Another source of the glueball-mass shift is its possible mixture with neighbouring $q\bar{q}$ -mesons. The last of these effects can be taken into account by working within the K-matrix technique.

The advantage of the K-matrix approach is its ability to analyze the structure of multichannel partial amplitudes of overlapping resonances. The K-matrix amplitude is unitary and correctly represents analytic properties on the right-hand side of the complex s -plane. Although this approach does not reproduce the analytic structure of the amplitude on the left-hand side of the s -plane, one may hope that this does not lead to significant inaccuracy in finding the pole positions and coupling constants in the mass region under consideration. Left-hand side singularities of the partial amplitude can be

taken into account in the framework of the multichannel dispersion relation N/D method: we consider this approach as a necessary though later step in the analysis of the 00^{++} amplitude.

K-matrix analysis demonstrates [8, 9] that poles of the partial amplitude (or physical poles which correspond to the observable states) are determined by the mixture of input states related to the K-matrix poles via their transition into real mesons. The wave function of a physical state is a mixture of not only the input states but also of real mesons, which realize this mixture and are responsible for the decay of the physical state. Because of this phenomenon, we call the input states "bare states", i.e. the states without a cloud of real meson. Decay coupling constants of bare states are fixed by their quark-gluon content [15, 16, 17]. So bare states can be classified by means of their couplings to different two-meson channels. We perform here such a classification of the bare states, f_0^{bare} , using the ratios of their coupling constants to the $\pi\pi$, $K\bar{K}$, $\eta\eta$, and $\eta\eta'$ channels in the leading terms of the $1/N_c$ expansion [18] (however, for the candidates for a glueball, the-next-to-leading terms will also be estimated). Our analysis gives evidence for the existence of two $q\bar{q}$ -nonets, while one bare state with mass around 1200-1600 MeV is superfluous in the $q\bar{q}$ -systematics. So, the analysis points to the scenario (b), limiting the mass of the exotic state to the range 1200-1600 MeV. Large coupling constants indicate that this superfluous bare state is dispersed over neighbouring physical states: the narrow $f_0(1300)$ and $f_0(1500)$ resonances and the broad $f_0(1530_{-250}^{+90})$.

1) K-matrix approach and quark combinatoric rules for the decay coupling constants

The standard K-matrix technique is used for the description of the meson scattering amplitudes in the 00^{++} -channel:

$$A = K(I - i\rho K)^{-1}, \quad (1)$$

where K_{ab} is a 5×5 matrix ($a, b = 1, 2, 3, 4, 5$), with the following notations for meson states: $1 = \pi\pi$, $2 = K\bar{K}$, $3 = \eta\eta$, $4 = \eta\eta'$ and $5 = \pi\pi\pi\pi$ + other multimeson states. The phase space matrix is diagonal: $\rho_{ab} = \delta_{ab}\rho_a$, with the following ρ_a :

$$\rho_a(s) = \sqrt{\frac{s - 4m_a^2}{s}}, \quad a = 1, 2, 3, \quad (2)$$

$$\rho_4(s) = \begin{cases} \sqrt{\left(1 - \frac{(m_\eta + m_{\eta'})^2}{s}\right) \left(1 - \frac{(m_\eta - m_{\eta'})^2}{s}\right)} & , \quad s > (m_\eta - m_{\eta'})^2 \\ 0 & , \quad s < (m_\eta - m_{\eta'})^2 \end{cases}.$$

Here $m_1 = m_\pi$, $m_2 = m_K$, $m_3 = m_\eta$. Phase space factors are responsible for the threshold singularities of the amplitude: to prevent the violation of analytic properties we

use analytic continuation for ρ_a below threshold. For example, the $\eta\eta$ phase space factor $\rho_a = (1 - 4m_\eta^2/s)^{1/2}$ becomes equal to $i(4m_\eta^2/s - 1)^{1/2}$ below the $\eta\eta$ threshold. The phase space factors we use lead to false kinematic singularities at $s = 0$ (in all phase space factors) and at $s \leq (m_{\eta'} - m_\eta)^2$ (in the $\eta\eta'$ space factor); but these false singularities (which are standard for the K-matrix approach) are rather distant from the investigated physical region. For multimeson phase volume at s below 1 GeV², we use the four-pion phase space defined either as $\rho\rho$ phase space or as $\sigma\sigma$ phase space. The result is practically the same in the two cases and we show the $\rho\rho$ phase space, for which formulae are simpler:

$$\rho_5(s) = \begin{cases} \rho_0 \int \frac{ds_1}{\pi} \int \frac{ds_2}{\pi} \frac{M^2 \Gamma(s_1) \Gamma(s_2) \sqrt{(s+s_1-s_2)^2 - 4ss_1}}{s[(M^2-s_1)^2 + M^2 \Gamma^2(s_1)][(M^2-s_2)^2 + M^2 \Gamma^2(s_2)]} & , \quad s < 1 \text{ GeV}^2 \\ 1 & , \quad s > 1 \text{ GeV}^2 \end{cases} \quad (3)$$

Here s_1 and s_2 are the two-pion energies squared, M is the ρ -meson mass and $\Gamma(s)$ is its energy-dependent width, $\Gamma(s) = \gamma \rho_1^3(s)$. The factor ρ_0 provides continuity of $\rho_5(s)$ at $s = 1 \text{ GeV}^2$.

For K_{ab} we use the parametrization similar to that of ref. [8]:

$$K_{ab}(s) = \left(\sum_{\alpha} \frac{g_a^{(\alpha)} g_b^{(\alpha)}}{M_{\alpha}^2 - s} + f_{ab} \frac{1 + s_0}{s + s_0} \right) \frac{s - m_{\pi}^2/2}{s} \quad , \quad (4)$$

where $g_a^{(\alpha)}$ is a coupling constant of the bare state α to the meson channel; the parameters f_{ab} and s_0 describe a smooth part of the K-matrix elements ($s_0 > 1.5 \text{ GeV}$).

The following formulae describe the GAMS $\pi\pi$, $\eta\eta$ and $\eta\eta'$ production amplitude due to t-channel exchange:

$$A_{\pi N \rightarrow N b} = N(\bar{\Psi}_N \gamma_5 \Psi_N) F_N(t) D(t) \tilde{K}_{\pi\pi(t),a} (1 - i\rho K)_{ab}^{-1} \quad , \quad b = \pi\pi, \eta\eta, \eta\eta' \quad ,$$

$$\tilde{K}_{\pi\pi(t),a} = \left(\sum_{\alpha} \frac{\tilde{g}^{(\alpha)}(t) g_a^{(\alpha)}}{M_{\alpha}^2 - s} + \tilde{f}_a(t) \frac{1 + s_0}{s + s_0} \right) \frac{s - m_{\pi}^2/2}{s} \quad , \quad (5)$$

$$\tilde{g}^{(\alpha)}(t) = g_1^{(\alpha)} + \left(1 - \frac{t}{m_{\pi}^2}\right) \left(\Lambda_g - \frac{t}{m_{\pi}^2}\right) g'^{(\alpha)} \quad ,$$

$$\tilde{f}_a(t) = f_{1a} + \left(1 - \frac{t}{m_{\pi}^2}\right) \left(\Lambda_g - \frac{t}{m_{\pi}^2}\right) f'_a \quad , \quad (6)$$

$$F_N(t) = \left[\frac{\tilde{\Lambda} - m_{\pi}^2}{\tilde{\Lambda} - t} \right]^4 \quad , \quad D(t) = (m_{\pi}^2 - t)^{-1} \quad . \quad (7)$$

Here $F_N(t)$ is the nucleon form factor and $D(t)$ is the pion propagator.

The part of the amplitudes $p\bar{p} \text{ (at rest)} \rightarrow \pi^0 \pi^0 \pi^0, \pi^0 \eta\eta$ which corresponds to the two-meson production in 00^{++} state $A_{p\bar{p} \rightarrow \text{mesons}} = A_1(s_{23}) + A_2(s_{13}) + A_3(s_{12})$ (where the

amplitude $A_k(s_{ij})$ stands for any interaction of particles in intermediate states but with last interactions when the particle k is a spectator) has the following form:

$$A_1(s_{23}) = \tilde{K}_{p\bar{p}\pi,a}(s_{23}) (1 - i\rho K)_{ab}^{-1} \quad , \quad b = \pi\pi, \eta\eta \quad ,$$

$$\tilde{K}_{p\bar{p}\pi,a}(s_{ij}) = \left(\sum_{\alpha} \frac{\Lambda_{p\bar{p}\pi}^{(\alpha)} g_a^{(\alpha)}}{M_{\alpha}^2 - s_{ij}} + \phi_{p\bar{p}\pi,a} \frac{1 + s_0}{s_{ij} + s_0} \right) \frac{s_{ij} - m_{\pi}^2/2}{s_{ij}} \quad . \quad (8)$$

The same part of the amplitude in the $p\bar{p}$ (*at rest*) $\rightarrow \pi^0\pi^0\eta$ reaction is described as:

$$A_1(s_{23}) = \tilde{K}_{p\bar{p}\eta,a}(s_{23}) (1 - i\rho K)_{ab}^{-1} \quad , \quad b = \pi\pi \quad ,$$

$$\tilde{K}_{p\bar{p}\eta,a}(s_{ij}) = \left(\sum_{\alpha} \frac{\Lambda_{p\bar{p}\eta}^{(\alpha)} g_a^{(\alpha)}}{M_{\alpha}^2 - s_{ij}} + \phi_{p\bar{p}\eta,a} \frac{1 + s_0}{s_{ij} + s_0} \right) \frac{s_{ij} - m_{\eta}^2/2}{s_{ij}} \quad . \quad (9)$$

Parameters $\Lambda_{p\bar{p}\pi}^{\alpha}$ and $\phi_{p\bar{p}\pi}$ ($\Lambda_{p\bar{p}\eta}^{\alpha}$, $\phi_{p\bar{p}\eta}$) may be complex magnitudes with different phases due to three particle interactions.

In the leading terms of the $1/N$ expansion, the couplings of the $q\bar{q}$ -meson and glueball to the two mesons are determined by the diagrams where gluons produce $q\bar{q}$ -pairs (see Figs. 1b, c). The production of soft $q\bar{q}$ pairs by gluons violates flavour symmetry: the direct indication of such a violation comes from the description of the multiparticle production in the central hadron collisions at high energies (see ref. [19] and references therein) and from radiative J/ψ -decays [17]. In these cases the production of strange quarks is suppressed by the same factor λ . The ratios of the production probabilities are $u\bar{u} : d\bar{d} : s\bar{s} = 1 : 1 : \lambda$, with $\lambda = 0.4 - 0.5$ [19], that makes it possible to calculate unambiguously the ratios of the decay coupling constants in the framework of the quark combinatoric rules. Previously, quark combinatorics were successfully applied to the calculation of the hadron production in high energy collisions [20, 21] and in the J/ψ -decay [22]. Extending this property to the decays of 00^{++} $q\bar{q}$ -mesons, one may calculate the ratios of coupling constants $f_0 \rightarrow \pi\pi$, $K\bar{K}$, $\eta\eta$, $\eta\eta'$, $\eta'\eta'$. They are given in Table 1 for $f_0 = n\bar{n} \cos \Phi + s\bar{s} \sin \Phi$, where $n\bar{n} = (u\bar{u} + d\bar{d})/\sqrt{2}$.

The glueball decay couplings in the leading terms of $1/N$ -expansion obey the same ratios as the $q\bar{q}$ -meson couplings, with the mixing angle $\Phi = \Phi_{glueball}$, where $\tan \Phi_{glueball} = \sqrt{\lambda/2}$ [9]. This is resulted from the two-stage decay of a glueball (see Fig. 1c): intermediate $q\bar{q}$ -state in the glueball decay is a mixture of $n\bar{n}$ and $s\bar{s}$ quarks, with the angle $\Phi_{glueball} = 25^\circ \pm 3^\circ$.

In Table 1 we also present the glueball couplings in the scheme of Fig. 1d: these couplings are suppressed by the factor $1/N_c$ as compared to that of Fig. 1c. Nevertheless, we take them into account in the analysis of f_0^{bare} considered here as candidates for a glueball. The normalization in Table 1 is done, following ref. [14], in such a way that the

sum of the couplings squared over all channels is proportional to the probability of the production of new quark pair, $(2 + \lambda)$:

$$\sum_{channels} G^2(c)I(c) = \frac{1}{2}G^2(2 + \lambda)^2, \quad \sum_{channels} g_G^2(c)I(c) = \frac{1}{2}g_G^2(2 + \lambda)^2. \quad (10)$$

Here $I(c)$ is the identity factor and $c = \pi^0\pi^0, \pi^+\pi^-, K^+K^-$ and so on (see Table 1). With this normalization $g_G/G \simeq 1/N_c$. Our experience of quark-gluon diagram calculations teaches us that the factor $1/N_c$ actually leads to a suppression of the order of 1/10: in the fitting procedure we impose a restriction $|g_G/G| < 1/3$.

We use the coupling constant ratios shown in Table 1 for the determination of the quark/gluonic content of f_0^{bare} . Justification of this procedure is seen in the multichannel N/D -method: the couplings of f_0^{bare} satisfy the same ratios as the decay couplings of resonances in the dispersion relation approach [14].

2) Fit of the data

The fitting procedure used here is the same as in ref. [9]. Complications are due to the additional channel, $\eta\eta'$, and to the new K-matrix pole near 1800 MeV. We investigate a necessity for this fifth pole, fitting the data with and without it. The result is that for the description of the $\eta\eta$ and $\eta\eta'$ spectra above 1700 MeV, the K-matrix pole at 1800 MeV is definitely needed. We check the two-pole structure of the K-matrix elements in the range 1200-1400 MeV, performing the fits in the two- and one-pole approximations. The results confirm the statement of ref. [9]: the K-matrix without two-pole structure fails to describe data in the region 1100-1500 MeV. The one-pole approximation does not give a satisfactory description of either the Crystal Barrel or GAMS data on the $\pi^0\pi^0$ spectra at large momentum transfer squared, t . The latter show a well defined peak at 1300 MeV which corresponds to the $f_0(1300)$ resonance (see Fig. 6).

In ref. [9] two types of solution were found. In the present analysis, which covers the region of higher masses, up to 1900 MeV, there also exist two groups of solutions which are actually the continuations of solutions obtained in [9]. In solution **I**, the mixing angle $\Phi(1810)$ is positive and the resonance $f_0(1780)$ is narrow: $\Gamma(1780) = 140 \pm 20$ MeV. In solution **II** $\Phi(1820)$ is negative while $\Gamma(1780) = 310 \pm 50$ MeV. Let us stress that the 00^{++} resonance in the region 1750-1800 MeV was seen in the four-pion system in the decay $J/\psi \rightarrow \gamma 4\pi$, and two different solutions also give either a narrow [23] or a broad [24] resonance, just as obtained here.

Our nonet classification will be based on the following two constraints:

- (1) the angle difference between nonet partners should be 90° ; for this value the corridor $90^\circ \pm 5^\circ$ is allowed in our analysis.
- (2) coupling constants g of Table 1 should be approximately equal to each other for nonet partners.

The conventional quark model requires the equality of the coupling constants g . But the energy dependence of the loop diagram of Fig. 1a, $B(s)$, may violate this coupling constant equality because of mass differences of the nonet partners. Coupling constants of the K-matrix contain an additional s -dependent factor as compared to the couplings obtained in the N/D-method: $g^2(K) \rightarrow g^2(N/D)/(1+B'(s))$ [14]. The factor $(1+B'(s))^{-1}$ affects mostly the low- s region due to the threshold and left-hand side singularities of the partial amplitude. Therefore, the coupling constant equality is mostly violated for the lightest 00^{++} nonet, $1^3P_0 q\bar{q}$. We allow for the members of this nonet $1 \leq g(1)/g(2) \leq 1.5$, where the notations 1 and 2 refer to different f_0^{bare} . For the $2^3P_0 q\bar{q}$ nonet members, we put $g(1)/g(2) = 1$.

In solution **I** the following variant of the nonet classification exists:

- I.** $f_0^{bare}(720)$ and $f_0^{bare}(1260)$ are 1^3P_0 nonet partners,
 $f_0^{bare}(1600)$ and $f_0^{bare}(1810)$ are 2^3P_0 nonet partners,
 $f_0^{bare}(1230)$ is a glueball.

For this variant the χ^2 values are given in the second column of Table 2, parameters are presented in Table 3 and the description of data is shown by dashed curves in Figs. 2-6.

Within solution **II**, two variants describe well the data set:

- II-1.** $f_0^{bare}(720)$ and $f_0^{bare}(1260)$ are 1^3P_0 nonet partners,
 $f_0^{bare}(1600)$ and $f_0^{bare}(1810)$ are 2^3P_0 nonet partners,
 $f_0^{bare}(1230)$ is a glueball;
II-2. $f_0^{bare}(720)$ and $f_0^{bare}(1260)$ are 1^3P_0 nonet partners,
 $f_0^{bare}(1230)$ and $f_0^{bare}(1810)$ are 2^3P_0 nonet partners,
 $f_0^{bare}(1600)$ is a glueball.

The χ^2 values for the solutions **II-1** and **II-2** are given in the third and fourth columns of Table 2. Parameters are presented in Table 4 (solution **II-1**) and in Table 5 (solution **II-2**) and the description of data is shown in Figs. 2-5 by dotted curves for the solution **II-1** and in Figs. 2-8 by solid curves for the solution **II-2**.

The t -dependent couplings obtained from GAMS data and the production constants for the solution **II-2** for the Crystal Barrel data are presented in Table 6.

In all the solutions the calculated branching ratios, $p\bar{p} \rightarrow 3\pi^0/\eta\eta\pi$, for the description of Crystal Barrel data are very close to the experimental value 3.2 ± 0.8 [5]:

$$\text{BR}(p\bar{p} \rightarrow \pi\pi\pi/\eta\eta\pi) = 2.85(\text{I}), 2.72(\text{II-1}), 2.80(\text{II-2}).$$

The imposing of combinatoric rules on the resonance coupling constants and nonet classification constraints does not significantly change the description of data as compared

to the fit with free couplings. Moreover, the use of quark combinatorics provides a good convergence to the fit, whereas the fit with free couplings has rather poor convergence, thus yielding serious problems in finding the main minimum of χ^2 .

3) Results

Our simultaneous K-matrix analysis of the 00^{++} -wave points to the existence of five bare states f_0^{bare} in the mass region below 1900 MeV. Only two of them are definitely $s\bar{s}$ -rich states: $f_0^{bare}(720)$ and $f_0^{bare}(1810)$. Therefore only two nonets below 1900 MeV can be constructed; the following variants of the nonet classification are possible:

1. $f_0^{bare}(720), f_0^{bare}(1260)$ 1^3P_0 nonet, $f_0^{bare}(1600), f_0^{bare}(1810)$ 2^3P_0 nonet;
2. $f_0^{bare}(720), f_0^{bare}(1260)$ 1^3P_0 nonet, $f_0^{bare}(1230), f_0^{bare}(1810)$ 2^3P_0 nonet;

Scalar mesons in the lightest 1^3P_0 $q\bar{q}$ -nonet are the same in both our solutions: $f_0^{bare}(720 \pm 100)$ and $f_0^{bare}(1260 \pm 30)$. The flavour content of $f_0^{bare}(720 \pm 100)$ and $f_0^{bare}(1260 \pm 30)$ almost coincides with the $n\bar{n}/s\bar{s}$ content of η and η' , correspondingly, that indicates the symmetry in interactions which are responsible for the formation of the lightest scalar/pseudoscalar $q\bar{q}$ -mesons.

In any variant one of the bare states, either $f_0^{bare}(1230)$ or $f_0^{bare}(1600)$, is superfluous for the $q\bar{q}$ systematics, and its coupling constants are in accordance with the relations for glueball decay.

It should be emphasized that our bare state does not correspond to a pure gluodynamic glueball of refs. [12, 13]: the bare state includes quark degrees of freedom, in particular the $q\bar{q}$ component (this problem is discussed in detail in ref. [14]). This means that the mass of $f_0^{bare}(1230)$ or $f_0^{bare}(1600)$ should not coincide with the mass obtained in Lattice calculations for the pure glueball: 1550 ± 50 MeV [12] and 1710 ± 40 MeV [13]. Quite the opposite, as is shown in ref. [14], an admixture of the $q\bar{q}$ component wants to reduce the mass of a pure glueball by 200-300 MeV. Therefore, according to our fit, one would expect the mass of the gluodynamic glueball in the region 1450-1600 MeV for the variant **1** or in the region 1700-1900 MeV for the variant **2**.

A principal question to our analysis is how many states are in the region 1200-1400 MeV. We have investigated the variant with only one bare state in this region: it makes the quality of the fit worse. The fit of the data set is based on the existence of three resonances (amplitude poles) in the region 1200-1600 MeV: two comparatively narrow, $f_0(1300)$ and $f_0(1500)$, and a broad one, $f_0(1530_{-250}^{+90})$; the interference of the broad resonance with narrow ones produces a wide variety of effects which are typical for the spectra investigated. In order to have these three resonances we need three bare states in the region 1200-1600 MeV.

Nevertheless, one may be sceptical about taking into consideration such a broad resonance like $f_0(1530_{-250}^{+90})$. Here we would like to emphasize the existence of a very important

phenomenon for overlapping resonances [14]: the mixing of these resonances increases the width of one state, thus simultaneously reducing the width of another one. In the case of the full overlap, the width of one state tends to zero while the width of the second state tends to the sum of the widths of initial states, $\Gamma_1 + \Gamma_2$. For three overlapping resonances, the width of two states tend to zero while the width of the third state accumulates the widths of all initial resonances, $\Gamma_{third} \simeq \Gamma_1 + \Gamma_2 + \Gamma_3$. This effect is quite similar to what is well known in atomic/molecular physics, namely, the repulsion of close levels. Here, in the case of poles in the complex plane, the repulsion has a tendency to increase/decrease the widths. This means that in the case of overlapping and mixing resonances it is inevitable to have at least one resonance with a large width. Our analysis shows that this effect happens exactly in the mass region 1200-1600 MeV.

Conclusion

We have performed a simultaneous analysis of all available data for the 00^{++} channel in the mass region up to 1900 MeV. Five bare states are found: four of them are members of $q\bar{q}$ -nonets, while one state is extra for $q\bar{q}$ systematics: its couplings to meson channels point out that it is a bare glueball state. This bare glueball state is dispersed over three real resonances, $f_0(1300)$, $f_0(1500)$, and $f_0(1530^{+90}_{-250})$.

Acknowledgements

We thank A.V.Anisovich, D.V.Bugg, L.G.Dakhno, S.S.Gershtein, A.A.Kondashov, A.K.Likhoded, L.Montanet and S.A.Sadovsky for useful discussions. VVA and AVS are grateful to the Russian Foundation for Fundamental Investigations (Grant N 96-02-17934) for financial support. AVS is grateful to the fellowship of INTAS grant 93-2492-ext; the work was carried out within the research program of International Centre for Fundamental Physics in Moscow.

References

- [1] D. Alde et al., Z. Phys. **C66** (1995) 375;
A.A. Kondashov et al., Proc. 27th Intern. Conf. on High Energy Physics, Glasgow (1994) 1407;
Yu.D. Prokoshkin et al., Physics-Doklady **342** (1995), 473;
A.A. Kondashov et al, Preprint IHEP 95-137, Protvino (1995).
- [2] F. Binon et al., Nuovo Cim. **A78** (1983) 313.
- [3] F. Binon et al., Nuovo Cim. **A80** (1984) 363.
- [4] V.V. Anisovich et al., Phys. Lett. **B323** (1994) 233.
- [5] C. Amsler et al., Phys. Lett. **B342** (1995) 433.
- [6] B. Hyams et al., Nucl. Phys. **B64** (1973) 134.
- [7] S.J. Lindenbaum and R.S. Longacre, Phys. Lett. **B274** (1992) 492;
A. Etkin et al., Phys. Rev. **D25** (1982) 1786.
- [8] V.V. Anisovich et al., Phys. Lett. **B355** (1995) 363.
- [9] V.V. Anisovich and A.V. Sarantsev, Phys. Lett. B., in press.
- [10] D.V. Bugg, A.V. Sarantsev and B.S. Zou, Nucl. Phys. **B**, in press.
- [11] L. Montanet et al. (Particle Data Group), Phys. Rev. **D** 50 (1994) 1173.
- [12] G.S. Bali et al., Phys. Lett. **B309** (1993) 378;
R. Gupta et al., Phys. Rev. **D43** (1991) 2301.
- [13] J. Sexton, A. Vassarino and D. Weingarten, Phys.Rev.Lett. **75** (1995) 4563.
- [14] A.V. Anisovich, V.V. Anisovich and A.V. Sarantsev, "The lightest glueball: Investigation of the 00^{++} wave in dispersion relation approach", to be published.
- [15] S.S. Gershtein, A.K. Likhoded and Yu.D. Prokoshkin, Z. Phys. **C24** (1984) 305.
- [16] C. Amsler and F.E. Close, Phys. Lett. **B353** (1995) 385;
- [17] V.V. Anisovich, Phys. Lett. **B364** (1995) 195.
- [18] G. t'Hooft, Nucl. Phys. **B72** (1974) 461;
G. Veneziano, Nucl. Phys. **B117** (1976) 519.
- [19] V.V. Anisovich, M.G. Huber, M.N. Kobrinsky and B.Ch. Metch, Phys. Rev. **D42** (1990) 3045.

- [20] V.V. Anisovich and V.M. Shekhter, Nucl. Phys. **B55** (1973) 455.
- [21] J.D. Bjorken and G.E. Farrar, Phys. Rev. **D9** (1974) 1449.
- [22] M.A. Voloshin, Yu.P. Nikitin and P.I. Porfirov, Yad. Fiz. **35** (1982) 1006; [Sov. J. Nucl. Phys. 35 (1982) 586].
- [23] D.V. Bugg et al., Phys. Lett. **353** (1995) 378.
- [24] V.V. Anisovich et al., "Resonances in $J/\psi \rightarrow \gamma(\pi^+\pi^-\pi^+\pi^-)$ ", Preprint PNPI-TH-59-1994-2001 (1994).

- Fig. 1.** Quark-antiquark loop diagram which determines the glueball width (a); diagrams for the decay of a $q\bar{q}$ -meson (b) and a glueball (c,d) into two $q\bar{q}$ -meson states.
- Fig. 2.** The $\pi\pi \rightarrow \pi\pi$ S -wave amplitude module squared [1]; the events are collected at the momentum transfer squared $|t| < 0.20 \text{ GeV}^2/\text{c}^2$. The solid curve corresponds to solution **II-2**, the dashed curve to solution **I** and the dotted one to solution **II-1**.
- Fig. 3.** The $\pi\pi \rightarrow K\bar{K}$ S -wave amplitude squared: data are taken from refs.[7]; the style of the curves is the same as in Fig. 2.
- Fig. 4.** The $\pi\pi \rightarrow \eta\eta$ S -wave amplitude squared [2], the style of the curves is the same as in Fig. 2.
- Fig. 5.** The $\pi\pi \rightarrow \eta\eta'$ S -wave amplitude squared [3], the style of the curves is the same as in Fig. 2.
- Fig. 6.** Event numbers *versus* invariant mass of the $\pi\pi$ -system for different t -intervals in the $\pi^-p \rightarrow \pi^0\pi^0n$ reaction [1]. The solid curves correspond to solution **II-2** and the dashed curves to solution **I**.
- Fig. 7.** Fit of the $\pi\pi$ angular-moment distributions in the final state of the reaction $\pi^-p \rightarrow n\pi^+\pi^-$ at 17.2 GeV/c [6]. The curve corresponds to solution **II-2**.
- Fig. 8.** $\pi^0\pi^0$ spectra: in the $p\bar{p} \rightarrow \pi^0\pi^0\pi^0$ reaction (a), in the $p\bar{p} \rightarrow \eta\pi^0\pi^0$ reaction (b); $\eta\eta$ spectra in the $p\bar{p} \rightarrow \pi^0\eta\eta$ reaction (c), $\eta\pi^0$ spectra in the $p\bar{p} \rightarrow \pi^0\pi^0\eta$ reaction (d). Curves correspond to solution **II-2**.

Table 1

Coupling constants given by quark combinatorics for a $q\bar{q}$ -meson decaying into two pseudoscalar mesons in the leading terms of the $1/N$ expansion and for glueball decay in the next-to-leading terms of the $1/N$ expansion. Φ is the mixing angle for $n\bar{n}$ and $s\bar{s}$ states, and Θ is the mixing angle for $\eta - \eta'$ mesons: $\eta = n\bar{n} \cos \Theta - s\bar{s} \sin \Theta$ and $\eta' = n\bar{n} \sin \Theta + s\bar{s} \cos \Theta$. In eq.(2) $g_1 = \frac{\sqrt{3}}{2}g \cos \Phi$, $g_2 = g(\sqrt{2} \sin \Phi + \sqrt{\lambda} \cos \Phi)/2$.

Channel	The $q\bar{q}$ -meson decay couplings in the leading terms of $1/N$ expansion (Fig. 1e)	Glueball decay couplings in the next-to-leading terms of $1/N$ expansion (Fig. 1f)	Identity factor in phase space
$\pi^0\pi^0$	$g \cos \Phi / \sqrt{2}$	0	1/2
$\pi^+\pi^-$	$g \cos \Phi / \sqrt{2}$	0	1
K^+K^-	$g(\sqrt{2} \sin \Phi + \sqrt{\lambda} \cos \Phi) / \sqrt{8}$	0	1
K^0K^0	$g(\sqrt{2} \sin \Phi + \sqrt{\lambda} \cos \Phi) / \sqrt{8}$	0	1
$\eta\eta$	$g \left(\cos^2 \Theta \cos \Phi / \sqrt{2} + \sqrt{\lambda} \sin \Phi \sin^2 \Theta \right)$	$2g_G(\cos \Theta - \sqrt{\frac{\lambda}{2}} \sin \Theta)^2$	1/2
$\eta\eta'$	$g \sin \Theta \cos \Theta \left(\cos \Phi / \sqrt{2} - \sqrt{\lambda} \sin \Phi \right)$	$2g_G(\cos \Theta - \sqrt{\frac{\lambda}{2}} \sin \Theta) (\sin \Theta + \sqrt{\frac{\lambda}{2}} \cos \Theta)$	1
$\eta'\eta'$	$g \left(\sin^2 \Theta \cos \Phi / \sqrt{2} + \sqrt{\lambda} \sin \Phi \cos^2 \Theta \right)$	$2g_G(\sin \Theta + \sqrt{\frac{\lambda}{2}} \cos \Theta)^2$	1/2

Table 2
 χ^2 values for the K-matrix solutions.

	solution I	solution II-1	solution II-2	Number of points
Crystal Barrel data [4, 5] $p\bar{p} \rightarrow \pi^0\pi^0\pi^0$ $p\bar{p} \rightarrow \pi^0\eta\eta$ $p\bar{p} \rightarrow \pi^0\pi^0\eta$	1.57 1.59 1.52	1.53 1.63 1.58	1.52 1.60 1.62	1338 1798 1738
CERN-Münich [6] data $\pi^+\pi^- \rightarrow \pi^+\pi^-$	1.82	1.88	1.88	705
New S-wave GAMS data [1] $\pi^+\pi^- \rightarrow \pi^0\pi^0$	1.18	1.39	1.42	68
t-dependent GAMS data [1] $0.00 < t < 0.20$ $0.30 < t < 1.00$ $0.35 < t < 1.00$ $0.40 < t < 1.00$ $0.45 < t < 1.00$ $0.50 < t < 1.00$	2.79 2.98 1.40 2.20 1.50 1.92	2.87 3.04 1.43 2.16 1.42 1.82	3.19 2.84 1.39 2.38 1.55 1.97	21 38 38 38 38 38
GAMS data [2, 3] $\pi\pi \rightarrow \eta\eta$ $\pi\pi \rightarrow \eta\eta'$	0.70 0.38	0.88 0.52	0.99 0.37	16 8
Brookhaven data [7] $\pi\pi \rightarrow K\bar{K}$	0.80	0.69	0.61	35

Table 3

Masses, coupling constants (in GeV) and mixing angles (in degrees) for the f_0^{bare} -resonances for solution I. The errors reflect the boundaries for a satisfactory description of the data.

	Solution I				
	$\alpha = 1$	$\alpha = 2$	$\alpha = 3$	$\alpha = 4$	$\alpha = 5$
M	$0.651^{+.120}_{-.030}$	$1.219^{+.045}_{-.030}$	$1.255^{+.015}_{-.045}$	$1.617^{+.010}_{-.045}$	$1.813^{+.040}_{-.040}$
$g^{(\alpha)}$	$1.432^{+.100}_{-.100}$	$0.612^{+.050}_{-.200}$	$0.955^{+.080}_{-.080}$	$0.567^{+.050}_{-.050}$	$0.567^{+.050}_{-.050}$
g_G	0	$-0.120^{+.050}_{-.080}$	0	0	0
$g_5^{(\alpha)}$	0	$0.874^{+.100}_{-.150}$	0	$0.661^{+.100}_{-.150}$	$0.557^{+.100}_{-.100}$
Φ_α	-68.5^{+15}_{-4}	25.0^{+15}_{-15}	16.5^{+8}_{-8}	-6.0^{+15}_{-17}	89^{+5}_{-15}
	$a = \pi\pi$	$a = K\bar{K}$	$a = \eta\eta$	$a = \eta\eta'$	$a = 4\pi$
f_{1a}	$0.505^{+.100}_{-.100}$	$0.056^{+.100}_{-.100}$	$0.494^{+.100}_{-.100}$	$0.438^{+.100}_{-.100}$	$-0.160^{+.100}_{-.100}$
	$f_{ba} = 0 \quad b = 2, 3, 4, 5$				
	$g_3^{(1)} = -0.185^{+0.045}_{-0.045}$		$g_4^{(1)} = -0.250^{+0.100}_{-0.100}$		$s_0 = 5^{+\infty}_{-2.5}$
II sheet under $\pi\pi$ and 4π cuts	Pole position $1.012^{+.008}_{-.008}$ $-i0.033^{+.008}_{-.004}$				
IV sheet under $\pi\pi$, 4π , $K\bar{K}$, $\eta\eta$ cuts	$1.301^{+.010}_{-.020}$ $-i0.108^{+.025}_{-.015}$		$1.504^{+.004}_{-.008}$ $-i0.064^{+.008}_{-.008}$	$1.443^{+.150}_{-.120}$ $-i0.553^{+.080}_{-.120}$	
V sheet under $\pi\pi$, 4π , $K\bar{K}$,	$1.810^{+.020}_{-.020}$ $-i0.112^{+.010}_{-.030}$				

Table 4
Masses, coupling constants (in GeV) and mixing angles (in degrees) for the f_0^{bare} -resonances for the solution II-1.

	Solution II-1				
	$\alpha = 1$	$\alpha = 2$	$\alpha = 3$	$\alpha = 4$	$\alpha = 5$
M	$0.651^{+.120}_{-.030}$	$1.220^{+.050}_{-.050}$	$1.252^{+.020}_{-.030}$	$1.572^{+.040}_{-.030}$	$1.820^{+.030}_{-.040}$
$g^{(\alpha)}$	$1.454^{+.100}_{-.150}$	$0.605^{+.050}_{-.200}$	$0.969^{+.080}_{-.080}$	$0.431^{+.050}_{-.050}$	$0.431^{+.050}_{-.050}$
g_G	0	$-0.125^{+.050}_{-.080}$	0	0	0
$g_5^{(\alpha)}$	0	$0.765^{+.100}_{-.150}$	0	$0.570^{+.100}_{-.100}$	$-0.604^{+.120}_{-.120}$
Φ_α	-67.6^{+15}_{-4}	25.0^{+25}_{-15}	17.4^{+8}_{-8}	23.8^{+15}_{-17}	-61.2^{+15}_{-15}
	$a = \pi\pi$	$a = KK$	$a = \eta\eta$	$a = \eta\eta'$	$a = 4\pi$
f_{1a}	$0.626^{+.100}_{-.200}$	$-0.016^{+.100}_{-.100}$	$0.463^{+.100}_{-.200}$	$0.496^{+.100}_{-.200}$	$-0.072^{+.150}_{-.100}$
	$f_{ba} = 0 \quad b = 2, 3, 4, 5$				
	$g_3^{(1)} = -0.148^{+0.050}_{-0.050}$		$g_4^{(1)} = -0.268^{+0.100}_{-0.100}$		$s_0 = 5^{+\infty}_{-2.5}$
II sheet under $\pi\pi$ and 4π cuts	Pole position $1.010^{+.008}_{-.008}$ $-i0.040^{+.006}_{-.008}$				
IV sheet under $\pi\pi$, 4π , $K\bar{K}$, $\eta\eta$ cuts	$1.302^{+.010}_{-.020}$ $-i0.117^{+.015}_{-.025}$ $1.495^{+.006}_{-.006}$ $-i0.061^{+.008}_{-.008}$ $1.530^{+.100}_{-.200}$ $-i0.585^{+.050}_{-.100}$				
V sheet under $\pi\pi$, 4π , $K\bar{K}$, $\eta\eta$ and $\eta\eta'$ cuts	$1.798^{+.020}_{-.020}$ $-i0.089^{+.030}_{-.040}$				
V sheet under $\pi\pi$, 4π , $K\bar{K}$, $\eta\eta$ and $\eta\eta'$ cuts	$1.798^{+.020}_{-.020}$ $-i0.089^{+.030}_{-.040}$				

Table 5
Masses, coupling constants (in GeV) and mixing angles (in degrees) for the f_0^{bare} -resonances for the solution II-2.

	Solution II-2				
	$\alpha = 1$	$\alpha = 2$	$\alpha = 3$	$\alpha = 4$	$\alpha = 5$
M	$0.651^{+.120}_{-.030}$	$1.219^{+.060}_{-.050}$	$1.251^{+.020}_{-.030}$	$1.559^{+.060}_{-.020}$	$1.821^{+.030}_{-.040}$
$g^{(\alpha)}$	$1.503^{+.100}_{-.200}$	$0.508^{+.060}_{-.120}$	$1.002^{+.060}_{-.100}$	$0.398^{+.070}_{-.040}$	$0.508^{+.060}_{-.120}$
g_G	0	0	0	$0.030^{+.040}_{-.030}$	0
$g_5^{(\alpha)}$	0	$0.673^{+.120}_{-.100}$	0	$0.528^{+.100}_{-.100}$	$-0.584^{+.120}_{-.120}$
Φ_α	-66.7^{+15}_{-4}	42.3^{+8}_{-25}	18.3^{+4}_{-8}	25.0^{+5}_{-20}	-52.7^{+10}_{-20}
	$a = \pi\pi$	$a = KK$	$a = \eta\eta$	$a = \eta\eta'$	$a = 4\pi$
f_{1a}	$0.524^{+.150}_{-.150}$	$-0.058^{+.100}_{-.100}$	$0.413^{+.100}_{-.120}$	$0.406^{+.150}_{-.100}$	$-0.178^{+.150}_{-.100}$
	$f_{ba} = 0 \quad b = 2, 3, 4, 5$				
	$g_3^{(1)} = -0.167^{+0.100}_{-0.100}$		$g_4^{(1)} = -0.251^{+0.100}_{-0.100}$		$s_0 = 5^{+\infty}_{-2.5}$
II sheet under $\pi\pi$ and 4π cuts	Pole position $1.012^{+.008}_{-.008}$ $-i0.033^{+.008}_{-.004}$				
IV sheet under $\pi\pi$, 4π , $K\bar{K}$, $\eta\eta$ cuts	$1.301^{+.010}_{-.020}$ $-i0.108^{+.025}_{-.0150}$		$1.504^{+.004}_{-.008}$ $-i0.064^{+.008}_{-.008}$	$1.443^{+.150}_{-.120}$ $-i0.553^{+.080}_{-.120}$	
V sheet under $\pi\pi$, 4π , $K\bar{K}$, $\eta\eta$ and $\eta\eta'$ cuts	$1.814^{+.015}_{-.025}$ $-i0.113^{+.010}_{-.030}$				

Table 6

The parameters of the $\pi\pi$, $\eta\eta$ and $\eta\eta'$ production amplitude $A_{\pi N \rightarrow Nb}$ and $p\bar{p}$ annihilation amplitude $A_k(s_{ij})$ for solution II-2. All values are given in GeV.

	$A_{\pi N \rightarrow Nb}$				
	$\alpha = 1$	$\alpha = 2$	$\alpha = 3$	$\alpha = 4$	$\alpha = 5$
$g^{(\alpha)}$	-0.027	0	0.019	0.016	0
	$a = \pi\pi$	$a = K\bar{K}$	$a = \eta\eta$	$a = \eta\eta'$	$a = 4\pi$
f'_a	-0.025	0.027	0	0	0
	$N = 474 \quad \tilde{\Lambda} = 0.204 \quad \Lambda_g = 2.46$				
	$A_k(s_{ij})$				
	$\alpha = 1$	$\alpha = 2$	$\alpha = 3$	$\alpha = 4$	$\alpha = 5$
$Re(\Lambda_{p\bar{p}\pi}^{(\alpha)})$	0.023	0.590	0.389	1	-0.100
$Im(\Lambda_{p\bar{p}\pi}^{(\alpha)})$	-0.387	-0.016	-0.430	0	-0.192
$Re(\Lambda_{p\bar{p}\eta}^{(\alpha)})$	1	-0.304	-0.171	0	0
$Im(\Lambda_{p\bar{p}\eta}^{(\alpha)})$	0	0.243	0.473	0	0
	$a = \pi\pi$	$a = K\bar{K}$	$a = \eta\eta$	$a = \eta\eta'$	$a = 4\pi$
$Re(\phi_{p\bar{p}\pi,a})$	-0.102	-0.190	0.071	0	0
$Im(\phi_{p\bar{p}\pi,a})$	-0.148	0.093	0.092	0	0
$Re(\phi_{p\bar{p}\eta,a})$	0.879	0.049	0	0	0
$Im(\phi_{p\bar{p}\eta,a})$	1.312	-1.558	0	0	0

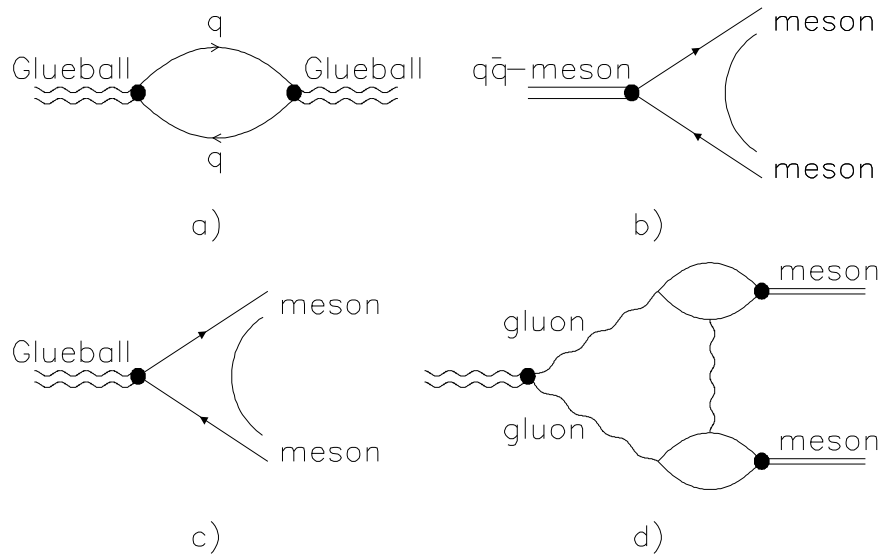


Fig. 1

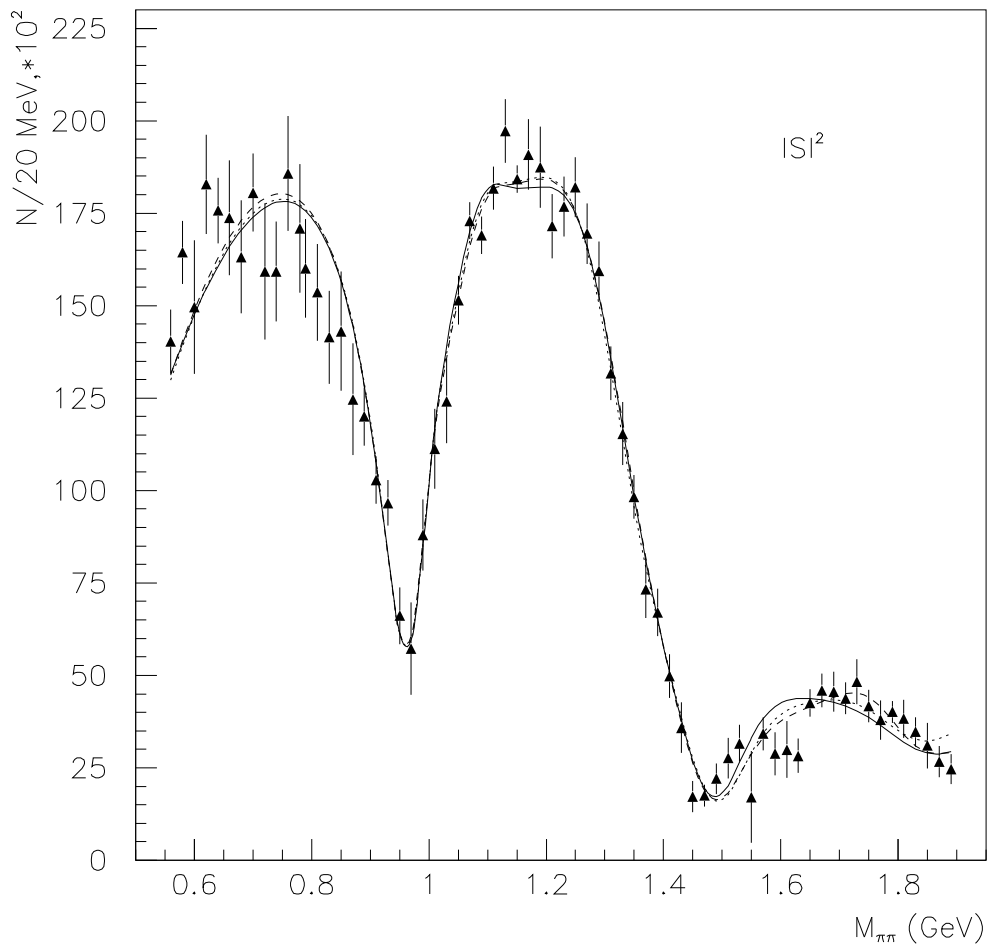


Fig. 2

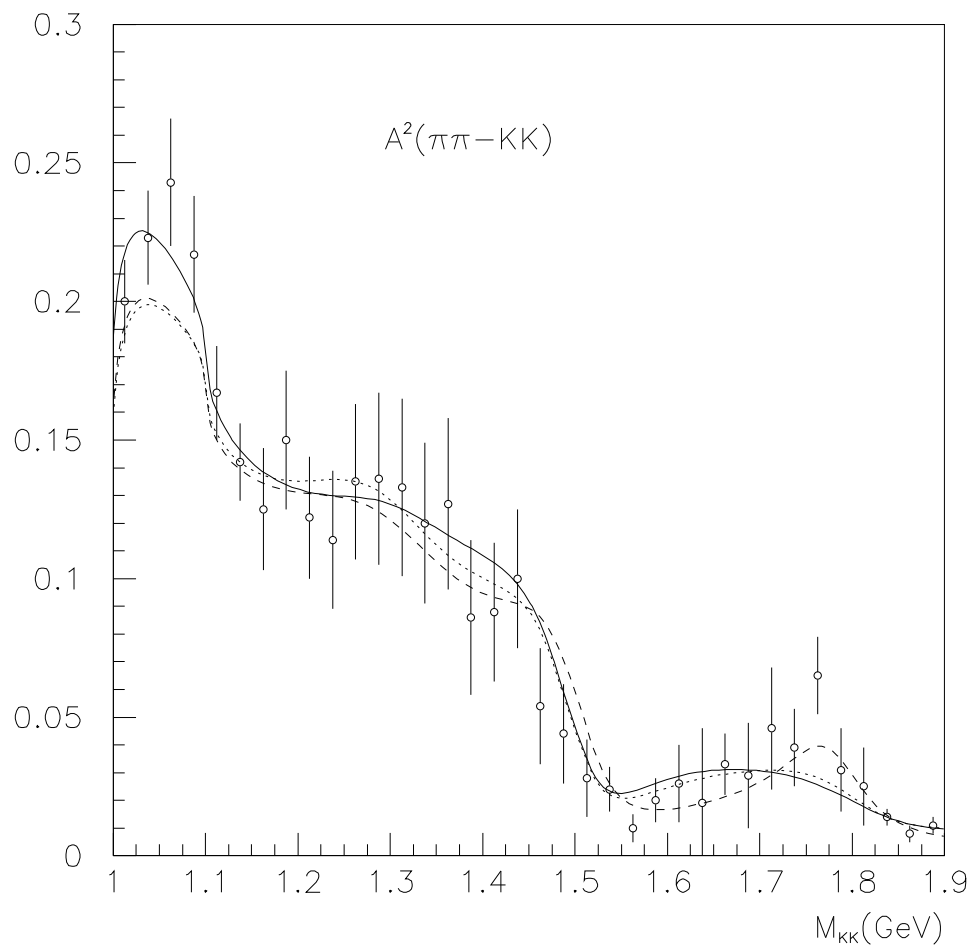


Fig. 3

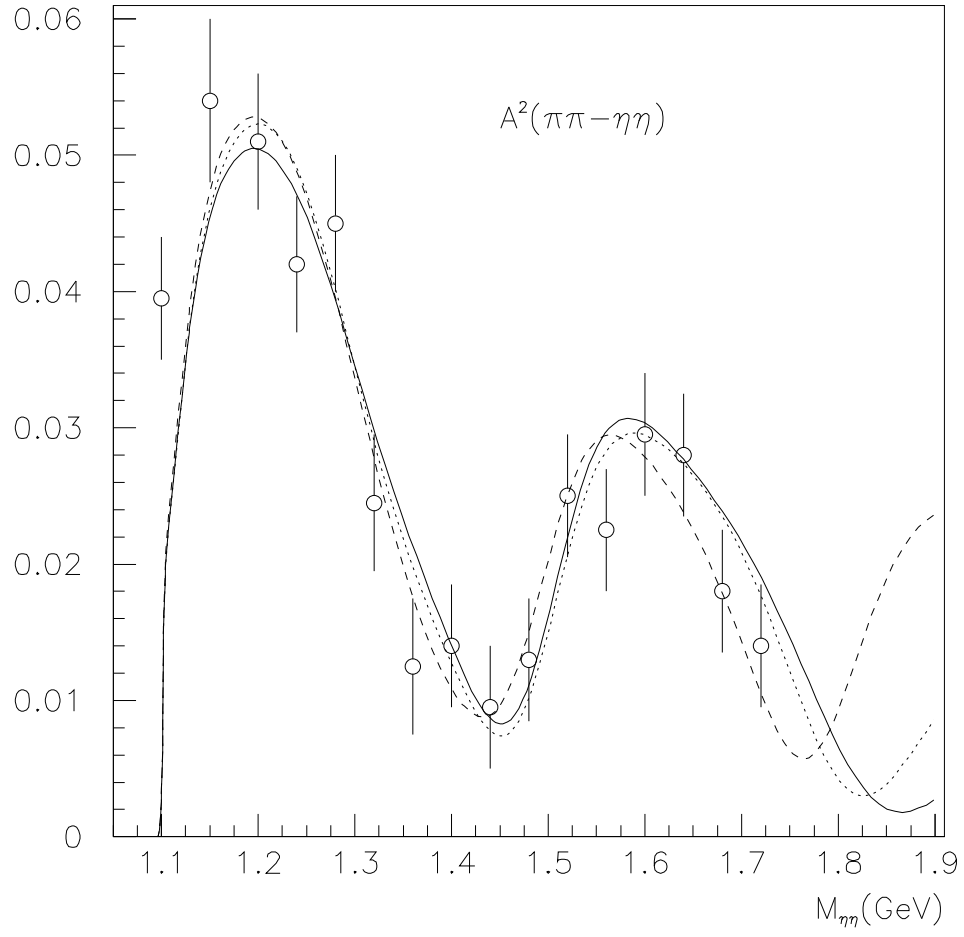


Fig. 4

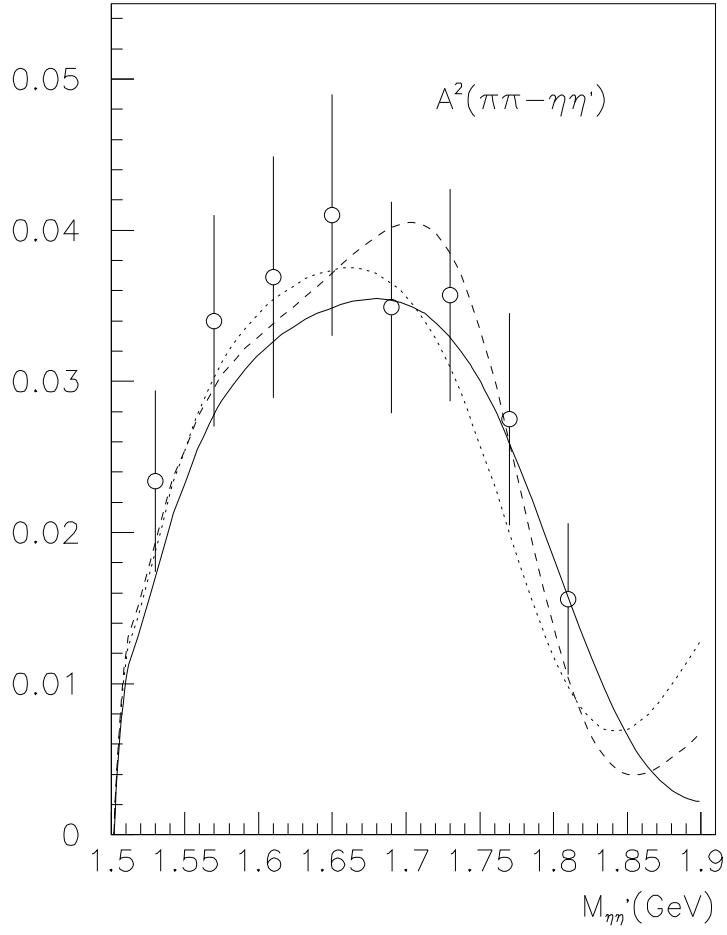


Fig. 5

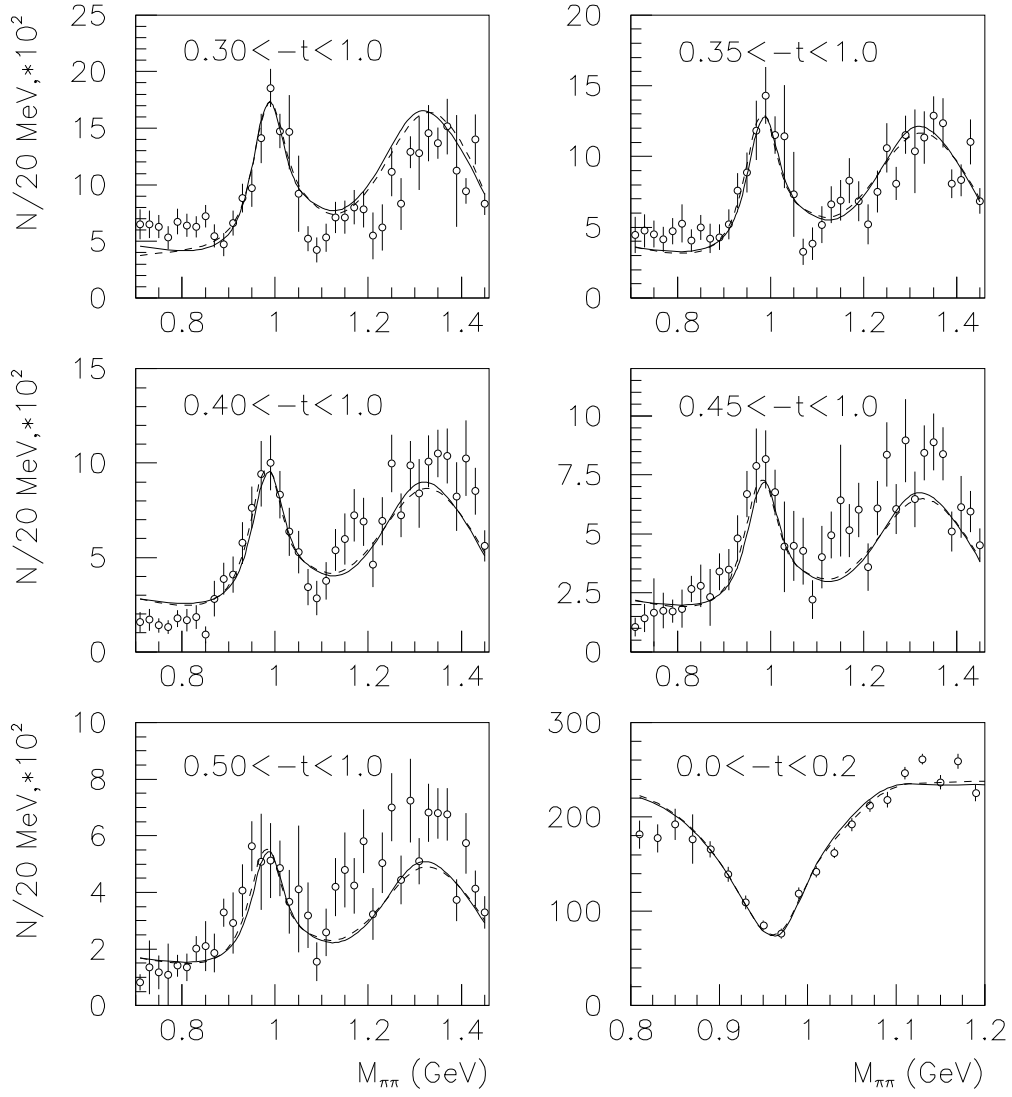


Fig. 6

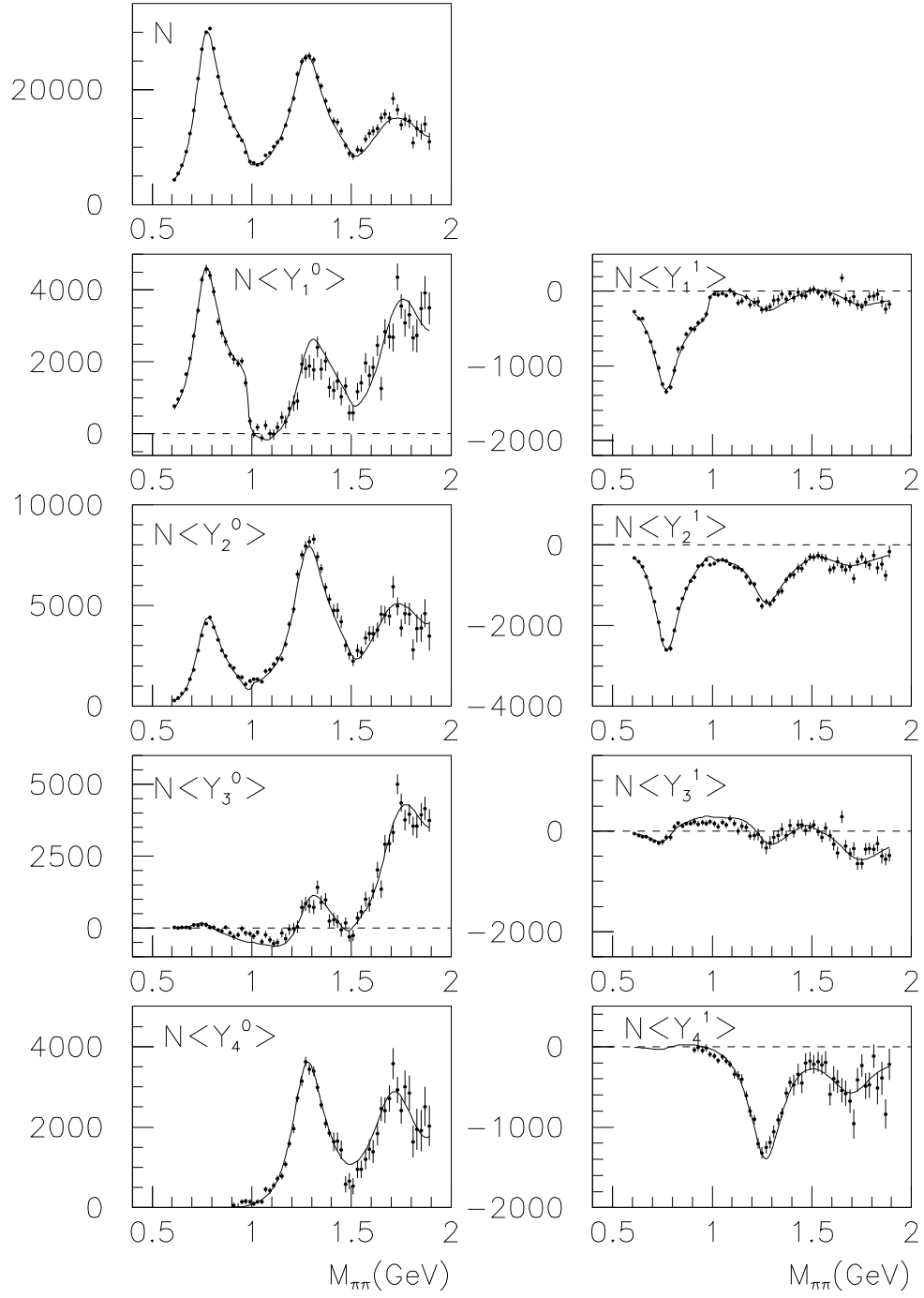


Fig. 7

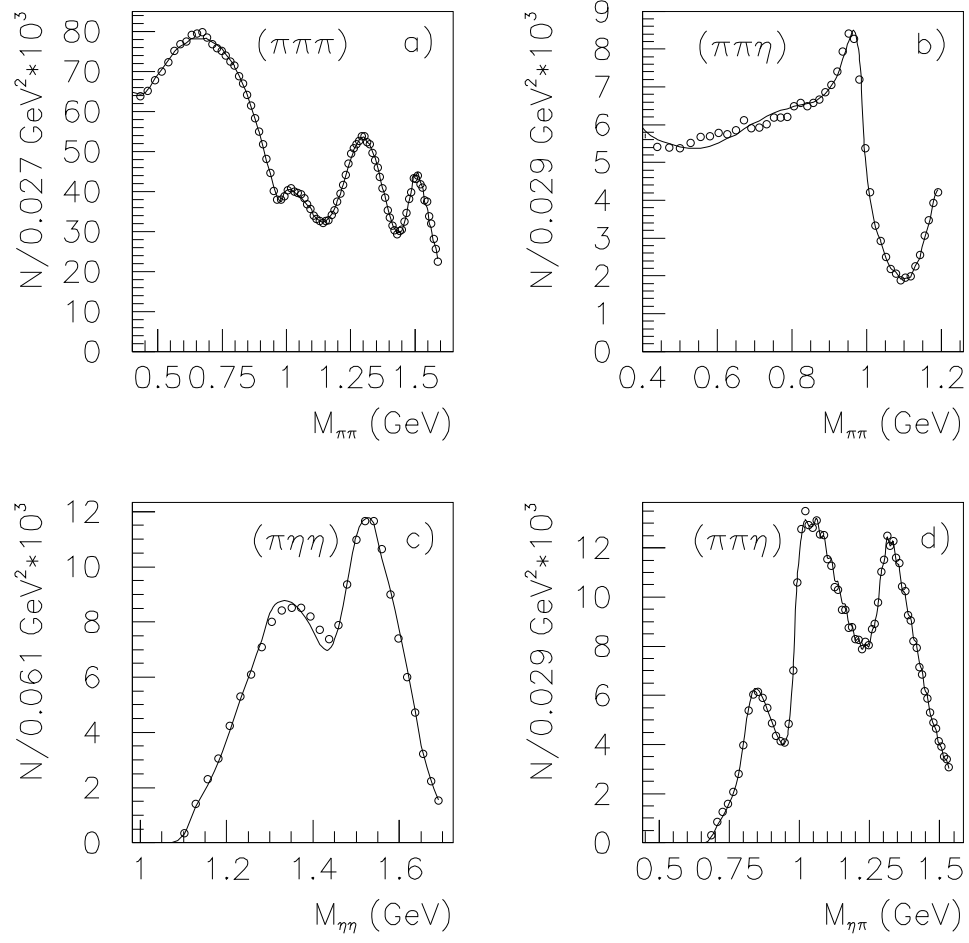


Fig. 8